Currents on the continental shelf adjacent to the Laje de Santos (SP, Brazil)*

*Roberto Fioravanti Carelli Fontes[1**], Belmiro Mendes de Castro[2]*

[1]Instituto de Biociências – Universidade Estadual Paulista
(Praça Infante Dom Henrique, s/n - Parque Bitaru - São Vicente - SP - 11330900 – Brazil)
[2]Instituto Oceanográfico – Universidade de São Paulo
(Praça do Oceanográfico, 191 – Butantã – São Paulo – SP – 05508120 – Brazil)

** Corresponding author: rcfontes@clp.unesp.br

ABSTRACT

Analysis of current meter data permitted the elaboration of a description of the hydrodynamic characteristics of the continental shelf adjacent to Laje de Santos, a rocky islet located in the inner part of the São Paulo Continental Shelf (SPCS). The currents in the region are mainly driven by the synoptic winds, presenting bidirectional motions approximately parallel to the local isobaths at all levels, depending on the wind direction but with the predominance of those that leave the isobaths to the left. The tidal currents in this sector of the SPCS are more energetic in the direction perpendicular to the isobaths in comparison with the along isobath component and have the predominance of the semidiurnal oscillations.

Descriptors: Currents, Continental Shelf, Laje de Santos, Southeast Brazil Continental Shelf.

RESUMO

A análise de dados correntográficos coletados em esforços observacionais recentes permitiu a descrição das características hidrodinâmicas da plataforma continental adjacente à Laje de Santos, situada na parte interna da Plataforma Continental de São Paulo (PCSP). As correntes nessa região são forçadas em primeira aproximação pelos ventos sinóticos, apresentando-se como movimentos bidirecionais quase paralelos às isóbatas em todos os níveis, dependentes da direção dos ventos, mas com predominância daqueles que deixam a isóbata à esquerda. As correntes de maré nessa parte da PCSP têm mais energia na direção perpendicular à isóbata, com predominância das oscilações semidiurnas.

Descritores: Correntes, Plataforma Continental, Laje de Santos, Plataforma Continental Sudeste.

Received: June 29, 2016
Approved: September 3, 2017
* Reference article of the Project MAPELMS - Environmental Monitoring of the State Marine Park of Laje de Santos

http://dx.doi.org/10.1590/S1679-87592017130206504

INTRODUCTION

The Lage de Santos (24.36°S, 46.17°W) is a rocky islet situated on the São Paulo Continental Shelf (SPCS), near the 35 m isobath, off the municipalities of the Baixada Santista (Figure 1). Due to the importance of this region to the marine ecosystem, the State Marine Park of Laje de Santos (SMPLS) was created on September 27, 1993 (Decree nº 37.537) to assure the total protection of these ecosystems. The SMPLS covers an area of approximately 50 km^2, including not only the Laje de Santos but also several submerged rock formations.

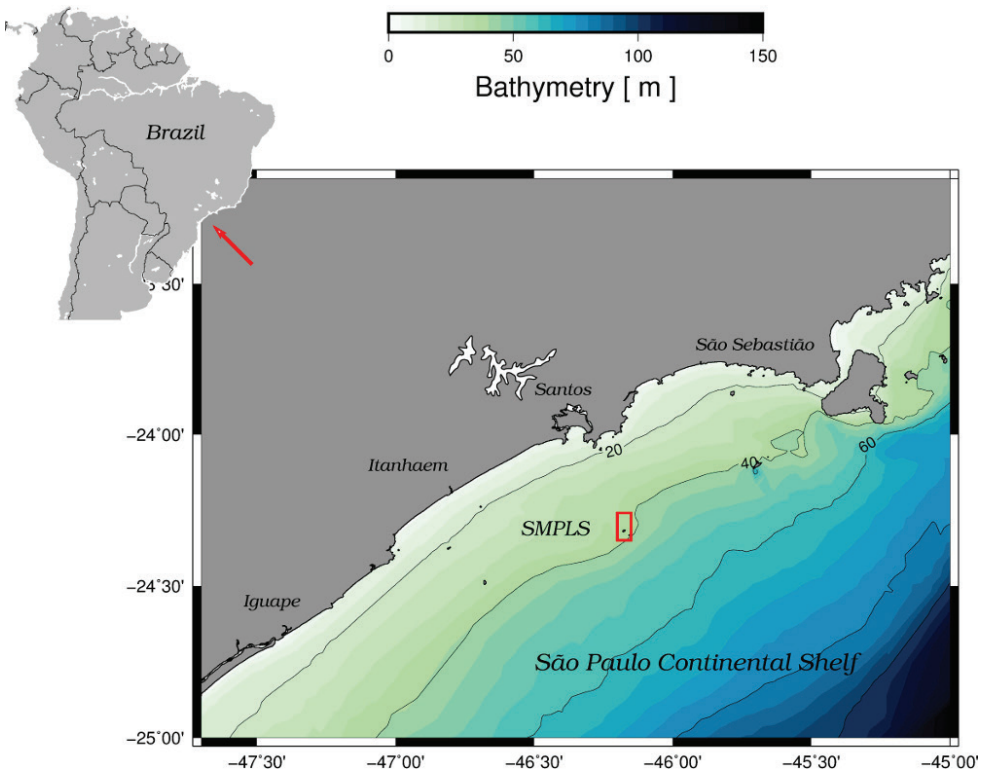

Figure 1. São Paulo Continental Shelf, highlighting the area of the State Marine Park of Laje de Santos (red rectangle). Bathymetry expressed in meters

The SPCS is part of the central region of the Southeast Continental Shelf (SECS), which is classified by LODER et al. (1998) as a wide shelf with a shelf-edge western boundary current. In the case of the SECS, the western boundary current is the Brazil Current (BC). The BC flows mainly over the continental slope along the shelf break carrying the Tropical Water (TW) in the mixed layer (at approximately 0 – 150m depth) and the South Atlantic Central Water (SACW) in the pycnocline (at approximately 150 – 500m depth). This type of continental shelf can be regionally divided, perpendicularly about the coast, into Inner Continental Shelf (ICS), Middle Continental Shelf (MCS) and Outer Continental Shelf (OCS).

Currents on the OCS of the SPCS are highly influenced by the average flow and the mesoscale variability of the BC (CASTRO; MIRANDA, 1998; SOUZA, 2000). On the ICS, even in the absence of large rivers, estuarine discharges create a pressure gradient that forces currents parallel to the coast in the N-NE direction, leaving the coastline to the left (COELHO, 2008; MAZZINI, 2009) and also generate small scale estuarine plumes. Throughout the extension of the SPCS, especially on the ICS and MCS, currents are driven by seasonal (annual time scale) and synoptic winds (time scale of a few days to a few weeks). These currents are in alignment with the isobaths and their directions depend on that of the wind. Particularly in the SMPLS, isobaths of 30 to 40 m bend towards the coast, in different alignment of the overall continental shelf.

Seasonal average winds reach the SPCS blowing from the NE-E to the SW-W since they constitute the

western part of the anticyclonic gyre of the South Atlantic Subtropical High (SASH). These winds drive currents flowing south- southwestwards with the coast to their right.

Weather frontal systems (cold fronts) are the factor primarily responsible for the synoptic variability of the wind field over the SPCS. These systems come from the south of the continent and move to the NW-NE along the SECS, bringing winds that blow from the S-SW towards the N-NE over the SPCS. The SPCS response to these winds is currents that flow north-northeastwards, leaving the coast to the left (DOTTORI; CASTRO, 2009).

On the supra-inertial motion scale, tides on the wide SPCS occur essentially as a co-oscillating response to tides from the adjacent deep sea (PEREIRA et al., 2007). The alignment between the co-phase lines of the more energetic tidal components (semidiurnal) and the coastal lines indicates that tidal currents on the SPCS flow perpendicularly to the isobaths and the coast. However, typical tidal currents on the SPCS have intensities of the order of centimeters per second while currents forced by the wind have intensities of the order of tens of centimeters per second.

Following the regionalization of the SPCS proposed by CASTRO (2014), the SMPLS is situated on the ICS (ICS-SP) mainly during autumn and winter, but can be located on the MCS (MCS-SP) during summer and spring. This regionalization is a function of the acting hydro-thermodynamic processes and is not associated with geomorphological features.

According to studies previously mentioned, the currents in the continental shelf are prevalently parallel to the coast, bidirectional and mainly driven by seasonal and synoptic winds, leaving the coast to the right in the former case and the left in the latter. Particularly in the SMPLS region, we find strong influences of current alignment due to isobaths distortions. Tidal currents have less kinetic energy than those generated by the wind and occur mostly perpendicularly to the coast. The analysis of current series also shows no dynamic influence of the BC in the SMPLS region.

Water masses found in the SMPLS area are a mixture of the already mentioned TW, characterized by high salinity ($S > 36$), the SACW, characterized by low temperatures ($T < 18°C$), and the Coastal Water (CW), that typically presents low salinities (CERDA; CASTRO, 2014; CASTRO, 2014).

Subsurface intrusions of the SACW towards the coast on the SPCS are common in summer and spring. During these seasons, the water mass is located closer to the coast and in contact with the ocean floor, leading to the formation of an acute seasonal thermocline in the SMPLS region. During winter and autumn, the SACW moves away from the coast, virtually suppressing the vertical stratification of density.

In this study, records from two ADCP moorings at distinct sites in SMPLS aim to explain the variability of local current direction and magnitude, as well as the typical time scales and its relationships with driving forces. The data was collected during the MAPEM-LS project (Environmental Monitoring of State Marine Park of Laje de Santos).

MATERIAL AND METHODS

Two acoustic Döppler current profilers (ADCP) were moored at LS^1 and LS^2, two different locations in the SMPLS area (Figure 2). Though current records occurred at different, but close periods, the analysis related to the wind records was taken at properly intervals and revealed interesting features from each location. The coordinates and period of the experiments at the two sampling points are shown in Table 1.

Table 1. Location and duration of the experiments to collect current meter data at the two sampling points, LS1 and LS2 (see Figure 1), of the MAPEM-LS project. Date format: dd/mm/yyyy; hour format: hh:mm.

POINT	LATITUDE	LONGITUDE	LOCAL DEPTH (m)	LAUNCHING-RECOVERY	START-END
LS1	24°18'55.2'S	46°09'44.6"W	39.3	29/08/2013, 10:24h-11/11/2013, 11:24h 11/11/2013, 12:11h--24/01/2014,10:31h 24/01/2014,13:04h-04/07/2014--12:34h 04/07/2014, 10:00h-30/09/2014, 12:00h	28/08/2013, 10:24h 04/07/2014, 12:34h
LS2	24°17'11.2"S	46°11'43.0"W	39.0	30/09/2014, 15:00h-18/12/2014, 10:00h 18/12/2014, 13:00h-11/06/2015, 12:00h	04/07/2014, 10:00h 11/06/2015, 12:00h

After correcting for the magnetic declination, current speed vectors were decomposed in alignment with the local reference isobaths, namely -45° and 90°, respectively to LS1 and LS2 moorings. Angles are in degree from North, and plus sign meaning clockwise.

The components of the speed vectors, obtained after the rotation of the coordinated axes, are designated as u (almost perpendicular to the local isobaths, $u > 0$ in the offshore direction) and v (almost parallel to the isobaths, $v > 0$ towards the left of $u > 0$). Hereinafter, the components u and v will be referred to as the perpendicular and parallel components, respectively. It is important to note that the 30 m and 40 m isobaths bend, where moorings were deployed. They have a N-S direction on a small scale. One must notice that LS1 were deployed between the Laje de Santos and a rocky formation (Figure 2). These are different features from the SPCS on a large scale, where the isobaths generally have a NE-SW direction (Figure 2).

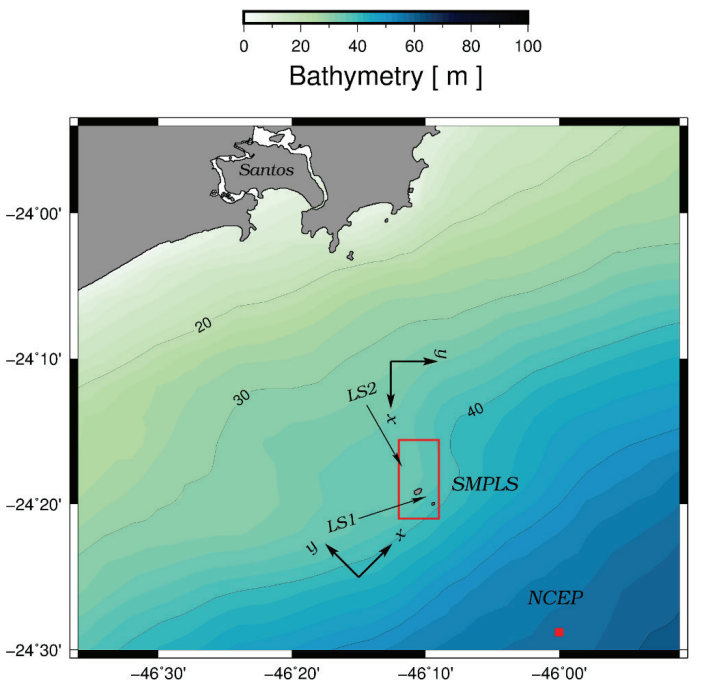

Figure 2. Bathymetric map of the region around the LS1 and LS2 moorings, highlighting the 30 m and 40 m isobaths. Axis x and y represent perpendicular and parallel directions to the isobaths, respectively. The NCEP point indicates the position of wind data.

A time series of surface winds was provided by NCEP/DOE Reanalysis-2 (KANAMITSU et al., 2002). These data have a sampling interval of 6h and original spatial resolution of 2.125°, which was later interpolated to a 0.5° resolution. The location of the NCEP/DOE point used is in Figure 2. The time series of the surface winds was analyzed from 08/29/2013 to 06/11/2016 and segmented according to the length of the time series of the current data obtained at LS^1 and LS^2. Since the synoptic winds have a spatial scale substantially larger than the scale of the bathymetric effects that occur at the LS^1 and LS^2 points, the wind speed vector was decomposed in the direction of maximum variance. MAZZINI (2009), who previously analyzed meteorological data collected on the Laje de Santos Isle, obtained the decomposition value of 54°, clockwise from the geographical north. A low-pass filter, Quadratic Lanczos type, with a cutoff frequency associated with a period of 33h, was applied to the "u" and "v" components of the current and wind time series. This procedure removes tidal oscillations and other high frequencies (WALTERS; HESTON, 1981) and therefore obtains sub-inertial (or subtidal) currents and winds. The inertial period in the region is approximately 29.1 h. The complex correlations between the wind and the current filtered time series were calculated following the method proposed by KUNDU (1976).

The energy spectra of the currents were obtained using the Welch method, which estimates the spectral energy density separating the time series into partially overlapping segments. Later, the method computes a modified periodogram for each segment and then calculates its average. The parameters used were: sampling frequency = 1h; segment length = 512; and attenuation coefficient of the Chebyshev spectral window = 50 dB.

Results

Currents measured at LS^1 (Figure 3) and LS^2 (Figures 4 an 5) visually exhibit an essentially barotropic behavior, i.e., the intensities and directions of the velocity vectors show a small variation throughout the water column (small vertical shear of the velocity vectors). From comparing the variance of their rotated components we find they are better aligned with local isobaths than the overall continental shelf orientation. Though currents were measured at several layers, only surface, intermediate and deep ones are shown.

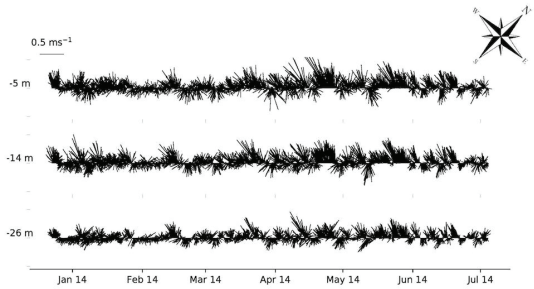

Figure 3. Time series of the current vectors measured at LS1, 24 January, 2014 to 4 July, 2014. The scale is indicated in the upper left corner. Vector direction is according to the wind rose in the upper right corner. Abscissa axis: time (mm/dd/yy). Ordinate axis: depth (m).

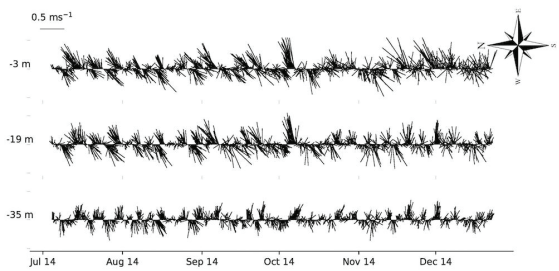

Figure 4. Time series of the current vectors measured at LS2 (July to December, 2014). The scale is indicated in the upper left corner. Vector direction is according to the wind rose in the upper right corner. Abscissa axis: time (mm/dd/yy). Ordinate axis: depth (m).

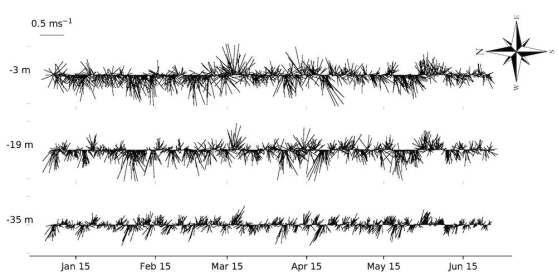

Figure 5. Time series of the current vectors measured at LS^2 (January to June, 2015). The scale is indicated in the upper left corner. Vector direction is according to the wind rose in the upper right corner. Abscissa axis: time (mm/dd/yy). Ordinate axis: depth (m).

The results of the statistical moments are in Tables 2 and 3.The average value of the "u" and "v" components at LS[1] and LS2 are small when compared to the extreme values measured. These differences, along with the relatively large standard deviations of the averages, indicate the high temporal variability of both velocity components.

The average perpendicular currents converge towards the coast at LS1 and diverge at LS[2]. On the other hand, the currents parallel to the coast (Table 3) have a preferred direction that leaves the isobaths to the left at all levels at both sampling points, though the average was also small compared to the standard deviation. These differences between the two velocity components, combined with the fact that in general the parallel components have extreme values and standard deviations, higher in magnitude than the perpendicular ones, suggest that the average advection measured occurs preferentially in the direction almost parallel to the coast, but with a convergence signal to the coast at LS[1] and a divergence signal at LS[2].

Table 2. First statistical moments of the component perpendicular to the isobaths (u) of the current speed vector at LS1 and LS2. Level = L (m); Minimum = Min (ms^{-1}); Maximum = Max (ms^{-1}); Average = Avg (ms^{-1}); Standard Deviation = SD (ms^{-1}).

	LS1				LS2			
L	**Min**	**Max**	**Avg**	**SD**	**Min**	**Max**	**Avg**	**SD**
-3.0	-	-	-	-	-0.60	0.67	0.04	0.16
-8.0	-0.72	0.61	-0.03	0.14	-	-	-	-
-19.0	-	-	-	-	-0.37	0.49	0.01	0.10
-23.0	-0.60	0.33	-0.04	0.10	-	-	-	-
-35.0	-0.46	0.45	-0.02	0.09	-0.22	0.25	0.01	0.06

Table 3. First statistical moments of the component parallel to the isobaths (v) of the current speed vector at LS1 and LS2. Level = L (m); Minimum = Min (ms^{-1}); Maximum = Max (ms^{-1}); Average = Avg (ms^{-1}); Standard Deviation = SD (ms^{-1}).

	LS1				LS2			
L	**Min**	**Max**	**Avg**	**SD**	**Min**	**Max**	**Avg**	**SD**
-3.0	-	-	-	-	-0.65	0.72	0.03	0.23
-8.0	-0.58	0.61	0.03	0.19	-	-	-	-
-19.0	-	-	-	-	-0.57	0.53	0.00	0.18
-23.0	-0.44	0.50	0.04	0.15	-	-	-	-
-35.0	-0.33	0.37	0.02	0.11	-0.38	0.39	0.01	0.13

The general characteristics of the currents at LS[1] confirm the higher number of events when the currents leave the isobaths to the left and converge towards the coast (Figure 5). Currents that flow in the SE-S direction, leaving the coast to the right, are also frequent at LS[1]. At LS[2], the currents also exhibit great polarization in the direction parallel to the coast (Figure 6 and 7). Overall, Figures 6 and 7 support the understanding that the advection is almost parallel to the local isobaths at LS[1] and LS[2].

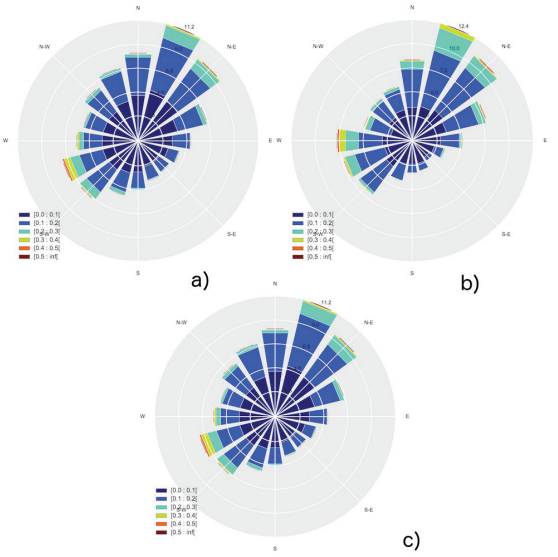

Figure 6. Directional histograms of the currents at LS1 on three levels: near the surface (-8 m; upper left panel - a), midwater (-23 m; upper right panel - b) and near the bottom (-35 m; lowest panel - c). Intensity ($m.s^{-1}$); direction (°, geographical coordinates); occurrence frequency (%).

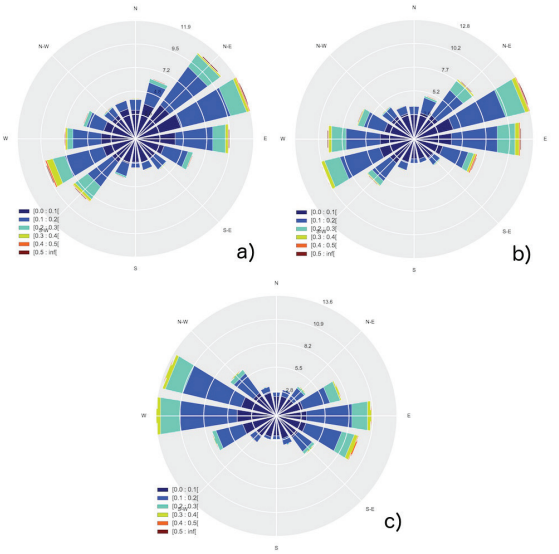

Figure 7. Directional histograms of the currents at LS2 on three levels: near the surface (–3 m; upper left panel - a), midwater (–19 m; upper right panel – b) and near the bottom (–35 m; lowest panel - c). Intensity (ms^{-1}); direction (°, geographical coordinates), occurrence frequency (%).

The variance of total perpendicular currents at LS1 and LS2 did not show substantial differences (Table 4). The same is observed for the filtered currents (sub-inertial). Generally, the supra-inertial energy oscillations of the currents at the two sampling points are greater than the sub-inertial oscillation in the perpendicular direction.

Table 4. Variances of the components perpendicular to the isobaths (u) of the current speed vector at LS1 and LS2 on the levels: near the surface (S), midwater (M) and near the bottom (B). Variance-Total was estimated from the original series and the Variance-Filtered was estimated from the filtered series (sub-inertial). Variance-Explained is the percentage ratio between Variance-Filtered and Variance-Total.

	VARIANCE - TOTAL ($m^2 s^{-2}$)	VARIANCE - FILTERED ($m^2 s^{-2}$)	VARIANCE- EXPLAINED (%)
LS1 – S	0.0188	0.0064	34.1
LS1 – M	0.0110	0.0052	47.0
LS1 – B	0.0077	0.0034	43.4
LS2 – S	0.0253	0.0142	56.0
LS2 – M	0.0096	0.0048	49.6
LS2 – B	0.0037	0.0015	40.9

The variances of total parallel currents (Table 5) indicate that the values at LS^2 are higher than those at LS^2. For these parallel components, the sub-inertial oscillations explain most of the total variance (more than 70%) at both sampling points. The variance of the parallel components are greater than the perpendicular ones (Tables 4 and 5), for both gross (total) and filtered series, in agreement with previous results that indicate currents are almost parallel to the isobaths. Furthermore, while the variability of the currents in the perpendicular direction is basically supra-inertial, in the parallel direction this variability is highly sub-inertial.

Table 5. Variances of the components parallel to the isobaths (v) of the current speed vector at LS1 and LS2 on the levels: near the surface (S), midwater (M) and near the bottom (B). Variance-Total was estimated for the original series and the Variance-Filtered was estimated for the filtered series (sub-inertial). Variance-Explained is the percentage ratio between Variance-Filtered and Variance-Total.

	VARIANCE - TOTAL ($m^2 s^{-2}$)	VARIANCE - FILTERED ($m^2 s^{-2}$)	VARIANCE- EXPLAINED (%)
LS1 – S	0.0357	0.0253	70.8
LS1 – M	0.0240	0.0207	86.3
LS1 – B	0.0132	0.0112	85.0
LS2 – S	0.0511	0.0380	74.4
LS2 – M	0.0331	0.0286	86.2
LS2 – B	0.0169	0.0146	86.6

The relative energy contained in the sub and supra-inertial oscillations can be compared by estimating the energy spectra from the current data series measured at approximately midwater (intermediate position between the surface and the bottom, Figures 8 and 9). These figures confirm that the parallel components contain more energy in the sub-inertial band than the perpendicular components, at both LS^1 and LS^2. In this band, higher energies appeared in the frequency range from 0.004 to 0.007 cph that correspond to periods between 6 and 10 days.

The frequencies associated with the semidiurnal tides (frequency of approximately 0.08 cph) are the most energetic for the parallel components of the speed vector in the supra-inertial band (Figures 8 and 9). An energy accumulation around the frequency of 0.04 cph, within the frequency band of the diurnal tide was also observed, especially for the components parallel to the coast. As the analyzed time series were too long, it was possible to separate in the spectrum the diurnal tide, with frequencies equal to or higher than 0.04 cph, from inertial oscillations, with frequencies between 0.03 and 0.04 cph, corresponding to periods near 28h.

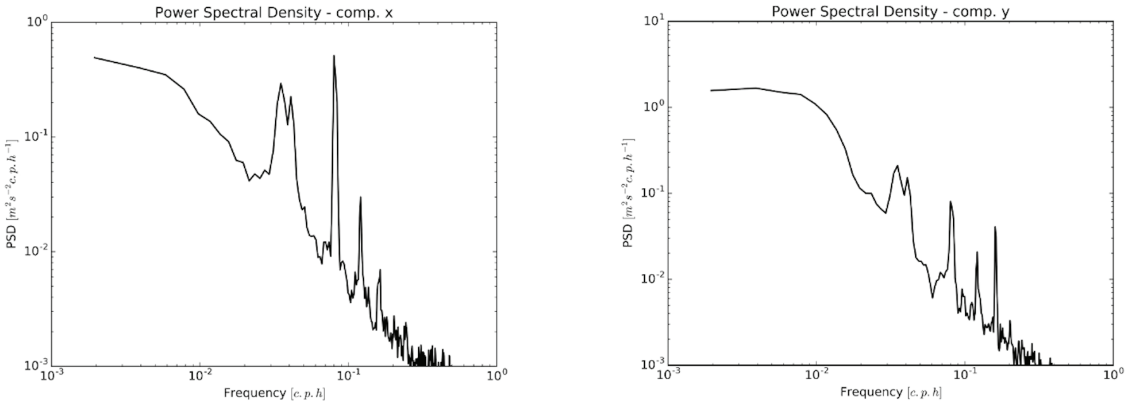

Figure 8. Energy spectrum (m^2 s^{-2} cph^{-1}) of the speed vector components normal (u, upper panel) and parallel (v, lower panel) to the isobaths observed at midwater at LS[1].

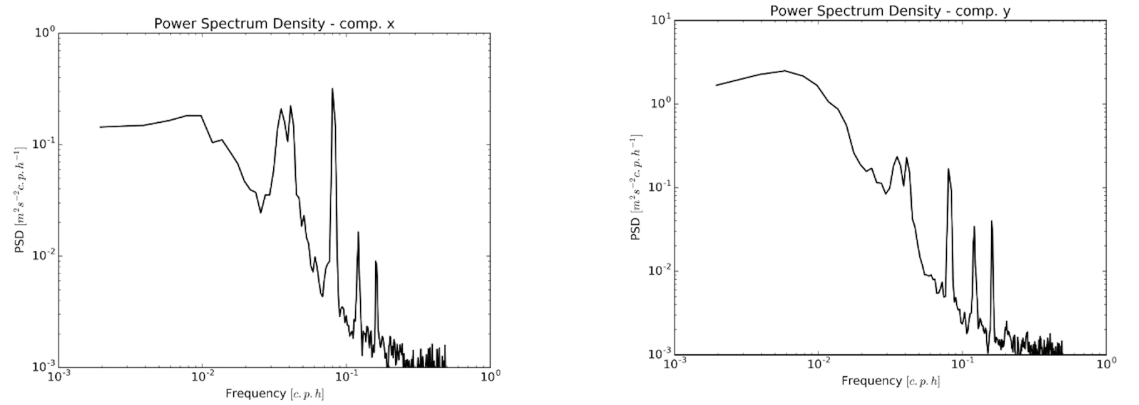

Figure 9. Energy spectrum (m^2 s^{-2} cph^{-1}) of the speed vector components normal (u, upper panel) and parallel (v, lower panel) to the isobaths observed at midwater at LS[2].

Especially on wide continental shelves like the SPCS, the sub-inertial variability of the currents is mostly driven by synoptic oscillations of the surface wind stress. This stress is proportional to the square of the wind speed. The directional histogram of the wind speed during the experiment period (Figure 10) shows clearly the predominance of easterly winds (i.e. blowing westwards), corresponding to times when there is a preponderant influence of the SASH, in the absence of cold fronts.

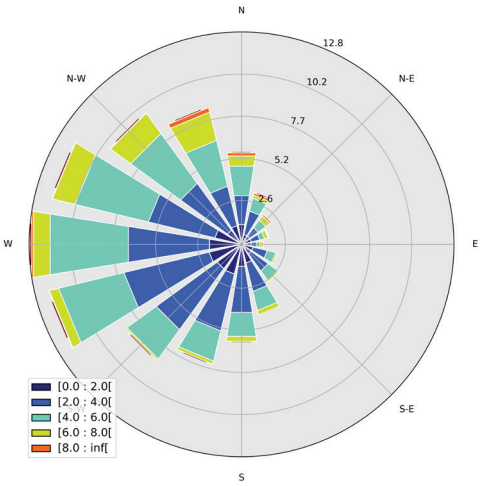

Figure 10. Directional histogram of the wind at the NCEP point. Intensity (ms^{-1}); direction (°, geographical coordinates); occurrence frequency (%).

Correlations between wind and current were calculated using the filtered series. Small-scale bathymetric features around the LS^1 and LS^2 points hinder the estimation of these correlations. Both the SASH and synoptic system winds have a much larger spatial scale and are not affected by the ocean bathymetry. Therefore, the correlations were estimated considering the wind and current vector series at both sampling points resulting in 0.40 and 0.54, respectively to LS^1 and LS^2. The amplitude of the correlations indicates statistically significant values, confirming the cause-effect relationship between the synoptic wind and the sub-inertial currents. Phase angles were 97° and -65° and reflect the preferential almost parallel to the isobath orientation of the currents, since the prevailing winds occur in the E-W direction.

Tidal variability of the currents can be better evaluated in the light of the results of a harmonic analysis, exemplified in Table 7 for the LS^1 mooring. In general, the semidiurnal components are the most energetic, with the predominance of the principal lunar (M^2). Of the diurnal components, K^1 has more energy than O^1, on all levels, and S^2, near the surface. Considering the semidiurnal components, it is noteworthy that they have more energy in the perpendicular (*u*) direction to the isobaths than in the parallel direction (*v*).

Table 6. Amplitude (10^{-2} ms^{-1}) of the components perpendicular (u) and parallel (v) to the isobaths of the tidal current speed vector at LS1 on the levels: near the surface (S), midwater (M) and near the bottom (B). The tidal components M2, S2, K1, O1 and M4 are the most energetic ones.

COMP.	M_2	S_2	K_1	O_1	M_4
U-S	4.72	3.22	3.97	0.31	0.12
U-M	5.25	3.24	1.16	1.16	0.36
U-B	4.87	3.07	0.83	0.84	0.37
V-S	1.80	1.57	2.88	0.82	1.10
V-M	1.66	1.32	1.30	0.61	1.39
V-B	1.48	1.26	0.84	0.04	1.14

DISCUSSION

The SMPLS region is situated on a wide continental shelf (SPCS) that presents a western boundary current at its edge. Continental shelf of this type has been classified and discussed by LODER et al. (1998). In general, western boundary currents have significant influence in its outer portion, transferring mechanical energy to the currents and mixing the water masses in it. In the case of the SPCS, the western boundary current is the Brazilian Current (BC). However, in the inner and middle portions of these continental shelves, such as the SMPLS, the hydro-thermodynamic influence of the western boundary currents is usually small. In these two regions, there is the dominance of responses of the continental shelf to winds, tides, and fluvial discharge stress forces.

The current results obtained at LS^1 and LS^2 confirm the appropriate classification by LODER et al. (1998) of the study region. The sub-inertial currents explained more than 70% of the observed variance in the parallel direction and less than 50% in the perpendicular direction (Tables 5 and 6). This means that the area in which LS^1 and LS^2 are set (on the ICS) exhibits responses typical of wide continental shelves to the wind and tidal forces. The synoptic variability of winds forces sub-inertial oscillations of currents in the parallel direction and the tidal co-oscillations dominate the currents in the perpendicular direction (Tables 5 and 6).

This different behavior between the two components of the velocity vector has also been observed by other authors on the ICS near the PEMSL (Mazzini, 1999). The author mentioned above also observed the high temporal variability of the sub-inertial parallel currents, with the preference for those leaving the isobaths to the left and regular periods between 6 and 11 days.

The preponderance of semidiurnal tidal currents in both directions, though with more energy in the perpendicular direction, has previously been observed by PEREIRA et al. (2007), when analyzing current meter data from the ICS of the SPCS.

The sub-inertial currents, substantially parallel to the isobaths, are driven by synoptic winds, as correlation results between currents and winds. This response, typical of inner portions of wide continental shelves, has previously been described in other regions of the SPCS (DOTTORI; CASTRO, 2009; MAZZINI, 2009).

CONCLUSIONS

The SMPLS region behaves hydrodynamically in agreement with the classification of LODER et al. (1998) in the inner and middle portions of wide continental shelves. Sub-inertial currents flow essentially parallel to the coast, driven by synoptic winds, bidirectional, oriented in such a way that the isobaths lie to their left. This direction, projected on a larger geographical scale than the

existing topographical features at LS^1 and LS^2, is from SW to NE. Supra-inertial tidal currents are more energetic in the direction perpendicular to the isobaths (than orthogonal), with the dominance of the semidiurnal components M^2 and S^2. The prevailing currents in LS^1 were 0.1 to 0.2 ms^{-1} N-NE and 0.1 to 0.2 ms^{-1} NE-E in LS^2. We found strong influences of current alignment caused by the 30-40 m isobaths retraction, towards the coast. Also, very local bathymetric nuances cause misalignment of currents, mostly in LS^1 and due to passages amongst rocky formations.

REFERENCES

CASTRO, B. M. Summer/winter stratification variability in the central part of the South Brazil Bight. *Cont. Shelf Res.*, 89: 15-23, 2014.

CASTRO, B. M.; Miranda, L. B. Physical Oceanography of the Western Atlantic Continental Shelf Located Between 4°N and 34°S. In: Robinson, A.L., Brink, K.H. (Org). *The Sea*, vol. 11. Oxford: John Wiley and Sons: 209-251, 1998.

CERDA, C.; Castro, B. M. Hydrographic climatology of South Brazil Bight shelf Waters between São Sebastião (24°S) and Cabo São Tomé (22°S). *Cont. Shelf Res*., 89: 5-14, 2014.

COELHO, A. L. Resposta da Plataforma Continental Sudeste a ventos sazonais e sinóticos de verão: estudos numéricos. 2008. Doctoral Thesis (Doutorado em Oceanografia Física) - Instituto Oceanográfico, Universidade de São Paulo, São Paulo, 2008. Available through <doi:10.11606/T.21.2008.tde-24062008-162856> [Accessed 10-14-2016, in Portuguese].

DOTTORI, M.; Castro, B. M. The response of the São Paulo continental shelf, Brazil, to synoptic winds. *Ocean Dynamics*, 59: 603-614, 2009

KANAMITSU, M.; EBISUZAKI, W.; WOOLLEN, J.; YANG, S–K.; HNILO, J. J.; FIORINO, M.; POTTER, G. L. NCEP-DOE AMIP-II Reanalysis (R-2). *Bull. Amer. Meteor. Soc.*, v. 83, p. 1631-1643, 2002.

KUNDU, P.K. Ekman veering observed near the ocean bottom. *J. Phys. Oceanogr.*, 6: 238-242, 1976.

LODER, J.W.; Boicourt, W. C.; Simpson, J.H. Western ocean boundary shelves: Coastal segment (W). In: *In: Robinson, A.L., Brink, K.H. (Org). The Sea, vol. 11. Oxford: John Wiley and Sons: 3-27, 1998.*

MAZZINI, P. L. F. Correntes subinerciais na Plataforma Continental interna entre Peruíbe e São Sebastião: observações. 2009. MSc. Dissertation (Mestrado em Oceanografia Física) - Instituto Oceanográfico, Universidade de São Paulo, São Paulo, 2009. Available through <doi:10.11606/D.21.2009.tde-22092009-154153> [Accessed 10-14-2016, in Portuguese].

PEREIRA, A. F.; Castro, B. M.; Calado, L.; Silveira, I. C. A. Numerical simulation of M_2 internal tides in the South Brazil Bight and their interaction with the Brazil Current. *J. Geophys. Res.*, 112: C04009, doi:10.1029/2006JC003673, 2007.

SOUZA, M. C. de ARRUDA. A Corrente do Brasil ao largo de Santos: medições diretas. 2000. MSc. Dissertation (Mestrado em Oceanografia Física) - Instituto Oceanográfico, Universidade de São Paulo, São Paulo, 2000. Available through <doi:10.11606/D.21.2000.tde-10092003-094250> [Accessed 10-14-2016, in Portuguese].

WALTERS, R.A; Heston, C. Removing the tidal-period variations from time-series data using low-pass digital filters. *J. Phys. Ocean*., 12: 112-115, 1982.